CR 137964
NAS2-7613

ROTOR DYNAMIC STATE AND PARAMETER IDENTIFICATION FROM HOVERING TRANSIENTS

Part II of Third Yearly Report under Contract NAS2-7613

Prepared for the Ames Directorate, USAAMRDL
at Ames Research Center, Moffett Field, California

by

K. H. Hohenemser

and

S. T. Crews

Department of Mechanical Engineering

Washington University
School of Engineering and Applied Science
St. Louis, Missouri 63130

June 1976

CR 137964

ROTOR DYNAMIC STATE AND PARAMETER IDENTIFICATION FROM HOVERING TRANSIENTS

Part II of Third Yearly Report under Contract NAS2-7613

Prepared for the Ames Directorate, USAAMRDL
at Ames Research Center, Moffett Field, California

by

K. H. Hohenemser

and

S. T. Crews

Department of Mechanical Engineering

Washington University
School of Engineering and Applied Science
St. Louis, Missouri 63130

June 1976

Preface to Third Yearly Report under Contract NAS2-7613

Work under Contract NAS2-7613 started on July 1, 1973. The research goals for a 3 year period stated in this contract are:

(a) Assess analytically the effects of fuselage motions on stability and random response. The problem is to develop an adequate but not overly complex flight dynamics analytical model and to study the effects of structural and electronic feedback, particularly for hingeless rotors.

(b) Study by computer and hardware experiments the feasibility of adequate perturbation models from non-linear trim conditions. The problem is to extract an adequate linear perturbation model for the purpose of stability and random motion studies. The extraction is to be performed on the basis of transient responses obtained either by computed time histories or by model tests.

(c) Extend the experimental methods to assess rotor wake-blade interactions by using a 4-bladed rotor model with the capability of progressing and regressing blade pitch excitation (cyclic pitch stirring), by using a 4-bladed rotor model with hub tilt stirring, and by testing rotor models in sinusoidal up or side flow.

Seven reports on the work under Contract NAS2-7613 have been submitted, references 1 to 7. Reference 1 completes research goal (a). References 2, 4, 6, 7 pertain to research goal (b). It is incomplete to date. References 3 and 5 pertain to research goal (c). It also is incomplete to date. Reference 3 presents the results of extensive frequency response tests. Reference 5 presents dynamic downwash

measurements in hovering during harmonic rotor excitation. Three manuscripts for publication have been prepared. The first has been published as reference 8. Two further manuscripts covering part of the material in references 3 and 7 have been submitted to journals.

The extensive rotor state and parameter identification work with computer simulated transients was found to be very useful for the subsequent data processing of the measured transients. It allowed to sort out possible inadequacies of the applied identification algorithm and of the inputs from possible inadequacies of the measurements and of the applied mathematical rotor model. Rotor state and parameter identifications from measured transients are presently complete for hovering conditions using cyclic pitch stirring transients. They are presented in reference 7. The corresponding work for forward flight conditions and for hub tilt stirring is planned to be completed in FY 1977 during an authorized extension of the research contract. It is also planned to refine the analytical rotor model used for the state and parameter identifications to include blade flexibility.

Rotor state and parameter identification from transients is still a field where little experience is available. As elaborated in Chapter 1 of reference 4 it takes four important ingredients to perform a successful state and parameter identification from transients; a suitable input, a suitable instrumentation for measuring key state variables, an adequate mathematical model of the system, and an efficient criterion function for the estimation algorithm. In all four respects considerable work had to be done in order to finally establish a combination of these four ingredients that led to success.

The lessons learned in this effort are hoped to pave the way for a wider application of rotor dynamic perturbation state and parameter identifications from transients about non-linear trim conditions, both in rotor wind tunnel testing and in rotor flight testing.

IV

ROTOR DYNAMIC STATE AND PARAMETER IDENTIFICATION FROM HOVERING TRANSIENTS

Part II of Third Yearly Report under Contract NAS2-7613

Abstract

State and parameter identifications based on a form of the maximum likelihood method are applied to the problem of extracting linear perturbation models including rotor dynamic inflow effects from transient blade flapping measurements. The estimation method is first studied in computer simulations and then applied to cyclic pitch stirring transients generated with a four-bladed rotor model operating in hovering trim conditions. The analytical perturbation models extracted from the transient test results are compared with transient and frequency response tests not used in the state and parameter identification. The identified analytical perturbation model is also compared with a simple theory. The method that is applicable both to small scale and full scale dynamic rotor testing is being extended to perturbations from forward flight trim conditions.

Table of Contents

Notation

A	aerodynamic blade constant, proportional to γ
F	Fourier coefficient
L	induced flow gain
M	information or sensitivity matrix
P	non-dimensional natural blade flapping frequency
R	rotor radius
a	blade section lift slope
h	rotor-to-ground plate distance
r	distance from rotor center
t	non-dimensional time (time of revolution 2π)
β	flapping angle, positive up
γ	blade Lock number
θ	up blade pitch angle
ν	down induced flow parameter, or innovation
σ	standard deviation, or rotor solidity ratio
$\bar{\sigma}$	standard deviation divided by mean value
τ	induced flow time constant
ω	non-dimensional pitch stirring frequency

Superscripts

$\cdot$	time derivative
$\hat{}$	estimate
$-$	trim or bias value
$*$	equivalent value

Notation (continued)

Subscripts

I, II	multiblade variables
o	mean value
m	measured variable
1ω	first Fourier coefficient

Introduction

Chapter 2 of reference 4 gives the results of state and parameter identifications based on computer simulated measurements of transients from hovering trim conditions. These simulation studies have been improved with respect to input design and data handling. The main progress, however, was made in using transient test data rather than simulated data for the identification of perturbation models for rotor hovering trim conditions. In previous experimental work the method of frequency response testing was used to obtain data on dynamic rotor inflow, see reference 3. During cyclic pitch stirring extensive zero advance ratio dynamic rotor wake measurements were obtained at a distance .2R below the rotor plane and are presented in reference 5, that also contains a description of the test set-up, the planned test procedures and the planned data handling systems for the subsequent cyclic pitch transient testing of the model rotor.

In the present report we discuss improvements in the test equipment and data handling made during the report year, present transient test results for hovering trim conditions, and compare the identified perturbation model with a simple theory and with the results of the preceding frequency response tests. Some transient test data have been obtained in the wind tunnel for forward flight trim conditions. Data processing for these tests is not completed as yet.

Further Simulation Studies

In Chapter 2 of reference 4 the maximum likelihood method of state and parameter identification is explained and applied to a perturbation model for hovering trim conditions developed in reference 8. A step input of cyclic pitch was applied at time t = 0. After the transient from the step input had almost subsided, pitch stirring with a constant stirring acceleration was initiated at t = 70, and the simulated test data between t = 70 and t = 82 were used for the state and parameter identification. It was found that better results are obtained for progressing cyclic pitch stirring than for regressing stirring. It was also found that the inclusion of the initial values for the flapping and inflow variables improved the results though at an increase in computer CPU time per iteration from 3.8 seconds to 6.3 seconds.

The system and measurement equations for perturbations from hovering trim conditions are given in reference 4 and will not be repeated here. We first applied these equations to the method of optimum data utilization developed in Chapter 3 of reference 4. Fig. 1 shows the relative standard deviations for the 3 parameters A, AL/τ, $1/\tau$ vs. time of the transient for a progressing pitch stirring acceleration of $\dot{\omega} = -.1/\pi$. The true values of the parameters are $A = .50$, $AL/\tau = .25$, $1/\tau = .125$. The assumed measurement noise in Gaussian with zero mean and a standard deviation of $\sigma(\beta_m) = .05$. The fourth identified parameter P (true value 1.2) was very rapidly and accurately identified and is not shown in Fig. 1. It is seen that a

transient time of t = 12 as used in reference 4 is inadequate while at t = 18 the standard deviations for all parameters have reached approximately their minimum asymptotic values. More data will not improve the accuracy of the parameters by any appreciable amount. Spot checks of identifications with various data lengths confirmed the characteristics shown in Fig. 1.

In order to avoid the identification of the initial conditions as was done in reference 4, the input was changed such that at the time of initiating the cyclic pitch stirring transient the cyclic pitch is zero. The input for $\dot{\omega} = -.1/\pi$ is represented by Fig. 2 in this report rather than by Fig. 2 in Chapter 2 of reference 4. The θ_I input is the same except for the extended time of the transient from t = 12 to 18. The θ_{II} input curve is shifted downward by 1.5 degrees in order to begin with the value zero. θ_I and θ_{II} were polluted by computer generated Gaussian noise with standard deviation $\sigma_\theta = .10$. The flapping response of blades 1 and 2 polluted by computer generated noise of standard deviation $\sigma_\beta = .05$ is shown in Fig. 3 This figure can be compared to Fig. 5 in Chapter 2 of reference 4. The two responses are quite different.

Table 1 gives for a time interval $\Delta t = .1$ used in the numerical integrations with the Runge-Kutta method and for a data length of t = 0 to 18 the results of 3 iterations. The value P = 1.20 was assumed given.

Table 1, P = 1.20

Parameter	A	AL/τ	1/τ
True Value	.500	.250	.125
Initial Estimate	.400	.200	.083
Iteration 1	.487	.243	.122
2	.492	.244	.121
3	.492	.244	.121
$M^{-1/2}$/Ident. Param.	.028	.13	.14

The iterations converge very rapidly to parameter values that are only little different from the assumed true values, taken from reference 8. Rapid convergence and small parameter errors were also found when the initial estimates differed much more from the true values than in the preceding table. The CPU time per iteration on the IBM 360/55 computer is 3.8 seconds, down from 6.3 seconds in cases with initial value identification in Chapter 2 of reference 4. Because of the modified input shown in Fig. 2 initial values of the perturbation state variables β_I, β_{II}, ν_I, ν_{II} are zero and need not be identified. The relative standard deviations for the parameters indicated in the last row are somewhat larger than in Fig. 1 for t = 18. The reason is that now θ_I and θ_{II} were also noise polluted, see Fig. 2, while Fig. 1 assumed noise pollution only in the simulated flapping measurements.

It also is of interest to identify the equivalent Lock number. Using the inputs of Fig. 2 and the simulated measurements of Fig. 3 one obtains the following 3 iterations

Parameter		A*
Initial Estimate		.400
Iteration	1	.280
	2	.272
	3	.271

Thus the equivalent Lock number is .271/.5 = .54 times the true Lock number.

Fig. 4 shows a comparison of the flapping responses for zero dynamic rotor inflow, for a dynamic inflow represented by the equivalent Lock number of .54 times the true value, and for the correct rotor dynamic inflow representation by L and τ. (A = .500, AL/τ = .25, $1/\tau$ = .125). Using the equivalent Lock number does improve the response as compared to that without inflow. However it does not properly represent the dynamic rotor inflow effects. Finally Fig. 5 shows the responses of the cyclic inflow variables v_I, v_{II} to the input of Fig. 2. These values are quite large and explain why omitting dynamic inflow leads to large response errors.

Improvements in Test Equipment and Data Handling

The acceleration for the cyclic pitch stirring electric motor had originally been measured in the horizontal position of the shaft. When the first series of 30 tests at 2°, 5°, and 8° collective pitch setting was evaluated it was found that the maximum likelihood identification method did converge as it did in the simulations. However,

the obtained parameters were in error. The blade Lock number converged to approximately its equivalent value rather than to its actual value, which made the values for L and τ meaningless. It was then discovered that the pitch stirring acceleration used for the tests was much smaller than anticipated from the preceding measurements. Apparently, changing the pitch stirring motor axis to the vertical position used for the pitch stirring tests largely reduced the acceleration.

Computer simulations were then conducted for the low pitch stirring acceleration of the test ($\dot{\omega} = .05/\pi$) and a duration of the transient from $t = 0$ to $t = 12$. The same identification difficulties occurred as for the test data, proving that the cause had been an inadequate input. Later it was found that low pitch stirring accelerations are adequate, if the length of the transient used in the parameter identification was sufficiently lengthened. The pitch stirring motor was then remounted so that the pitch stirring shaft is driven by a timing belt drive. The drive has a transmission ratio up to 1:7. Fig. 6 shows the input θ_{II} obtained for two pitch stirring accelerations used for the transient tests to be described in the next section. The identification length was extended to about 23 time units, since the pitch stirring acceleration is non-uniform and lower than average at the beginning of the transient.

Simultaneously with the modified pitch stirring drive the change-over from two differential blade flapping measurements to four separate blade flapping measurements was made. This required the installation of a new 20-ring slip ring assembly. As mentioned in reference 5 this modification had been planned for the forward flight transient tests.

Data processing of the transients revealed inaccuracies in the azimuth measurements of the pitch stirring and rotor shafts. These inaccuracies were mainly caused by the resolver wave shapes that substantially deviated from a harmonic function. After reshaping the resolver wave form by empirically finding an optimum filter and excitation frequency the azimuth errors were reduced. Removing an electric interference between the resolvers further improved their accuracy.

A rather strong 2 per rev. oscillation was observed in the hovering blade flapping measurements prior to the transient. It was found after considerable experimentation that this phenomenon could be substantially reduced by correcting non-uniformities of pre-lag and pre-flap angles between the individual blades.

As compared to the procedure described in reference 5 a number of modifications were made in the data processing. The entire data processing and state and parameter identification program was reformulated for use on the PDP-8 and PDP-12 mini computer complex that was programmed to perform all necessary data manipulations; digitizing the analogue data, transformation from rotating to fixed coordinates, separating the transient perturbation values from the trim values, executing the maximum likelihood algorithm to obtain the unknown parameter estimates, and generating analytical responses based on the identified parameters. This avoids manual key punching and is also more cost effective, since 20% usage time for the PDP-8 and PDP-12 mini computer complex could be bought under favorable conditions. The core memory of the complex had recently been increased from 16k to 38k which proved to be adequate for the task at hand.

The identification program was modified to apply to the parameters A, L, τ separately, rather than in combination. Although the individual iteration requires somewhat longer computer time, the convergence was found to improve, thus saving overall computer time. The identification program was further modified by considering the multiblade flapping variables as measured quantities and by introducing unknown biases to be identified for these variables. Thus the innovation is now given by

$$\nu = \begin{bmatrix} \beta_{Im} - \hat{\beta}_I - \bar{\beta}_I \\ \beta_{IIm} - \hat{\beta}_{II} - \bar{\beta}_{II} \end{bmatrix} \tag{1}$$

where $\bar{\beta}_I$ and $\bar{\beta}_{II}$ are the unknown biases. This method has the advantage that the transformation from single blade flapping angles to multiblade variables needs to be performed only once for the measured quantities, and not for each iteration.

The identification algorithm was expanded to include the parameter P(blade flapping frequency when rotating). In this form all parameters in the analytical model are identified. It was found that such a complete identification from test transients is possible and leads to P-values within a few percent of the predicted values. For the routine identification runs, P was then assumed to be given.

The identification algorithm was further modified to include for each iteration the updated measurement error covariance matrix obtained from the differences between the experimental data and those predicted

with the parameters for the preceding iteration: It was found that better convergence is obtained if only the diagonal terms of the measurement error covariance are used as "weights" for the criterion function used in the subsequent iteration. The updated measurement error covariance matrix is used also in the determination of the Cramér-Rao lower bound $M^{-1/2}$ for the parameter estimates, which thus becomes more meaningful.

The effect of transient duration on the parameter identifications was not only studied for the simulations but also for the tests. It was found that for good convergence and data fit a minimum data length of about 23 time units is required as indicated in Fig. 6. This is somewhat more than the 18 time units necessary according to Fig. 1 for simulations for a cyclic pitch stirring acceleration of $\dot{\omega} = -.1/\pi$.

Transient Test Results

The test conditions extended over the entire collective pitch range up to stall and covered three rotor-to-ground plate distances of 1.28R, 1.02R, and .78R. Only one example of intermediate steps in the identification process will be given here in form of Table 2. The collective pitch setting is 6.3°, the time interval between data points is .1. As indicated in Fig. 6 the identification was performed with the transient between t = 0 and t = 23. The blade flapping frequency is P = 1.17. The last column $((\sigma^2_{\beta I} + \sigma^2_{\beta II})/2)^{1/2}$ is a measure of the overall agreement between analytical and test data. The last row gives the diagonal terms of $M^{-1/2}$ indicating the parameter standard deviation (Cramér-Rao lower bound) for iterations 2 to 4.

Table 2 $P = 1.17$, $\theta_o = 6.3°$

Iteration	L	τ	$\bar{\beta}_I$	$\bar{\beta}_{II}$	A	$((\sigma^2_{\beta I} + \sigma^2_{\beta II})/2)^{1/2}$
0	6.00	8.00	0	0	.600	.0668
1	4.30	3.57	.025	.025	.395	.0276
2	4.35	4.38	.026	.023	.394	.0253
3	4.46	4.59	.026	.022	.392	.0253
4	4.44	4.60	.026	.022	.391	.0253
$M^{-1/2}$	.08	.16	.001	.002	.007	

The accuracy of the analytical as compared to the test data, $((\sigma^2_{\beta I} + \sigma^2_{\beta II})/2)^{1/2}$, does not change beyond the second iteration, though small parameter changes still occur.

Fig. 6 shows the input θ_{II}, whereby the solid line refers to the case of Table 2, the dash line to a higher cyclic pitch stirring acceleration. The θ_{II} values of Fig. 6 are normalized to an amplitude of one. The actual cyclic pitch amplitude was 1.4°. Fig. 7 shows for the time from t = 0 to t = 23 the flapping responses β_I and β_{II} to the normalized input from Fig. 6. The complete analytical model with identified A, L, τ (solid line) fits the test results (crosses) very well. An identification of the equivalent A = A* resulted in the value A* = .19. The response for this simplified analytical model (dash-dot line) shows some errors as compared to test data. Merely omitting the dynamic rotor inflow and retaining the correct value of A leads to a flapping amplitude (dash line) that is about twice the correct value .

In addition to comparing the analytical and test responses for the transient used in the parameter identification, it is of interest to perform such a comparison also for other transients. Fig. 8 refers to a transient with a higher acceleration for which the input is shown in Fig. 6 as dash line. While the trend is the same as discussed for Fig. 7, the agreement between analytical and test data is less satisfactory. In part this is caused by the fact that the bias errors for the measurements have not been removed as they were for the preceding test. The discrepancies become greater as the cyclic pitch stirring frequency increases. This may be caused by the neglected unsteady aerodynamics. The transient shown in Fig. 8 extends to a cyclic pitch stirring frequency of about 3 times the rotor rotational frequency in the fixed coordinate system. It is obviously not possible to cover this entire frequency range with the same set of L and τ parameters. This becomes evident also From Fig. 9 that shows the comparison between analytical and test results for the slow transient beyond the time 23. The test data in this time region have not been used for the parameter identification and the frequencies in this region are much higher than in the time region from 0 to 23 units. Fig. 10 shows the computed induced inflow v_I and v_{II} for the slow transient. A comparison with test data is not possible, but this figure gives an indication of the substantial magnitude of the dynamic inflow that is of the same order of magnitude as the inputs θ_I and θ_{II}.

In all transients the parameter A was identified close to $A = .39$. The results for L and τ are shown in Fig. 11, that summarizes all test

results obtained. The effect of the rotor-to-ground plate distance is masked by the scatter in the identified L and τ values.

Comparison with Theory

A simple momentum theory of dynamic rotor induced flow is presented in reference 9. It is based on the assumption that the axial induced flow is uniform over the disk and that the harmonic induced flow varies linearly with the radial distance from the rotor center. The air mass participating in the angular pitching and rolling motion is determined from potential flow theory about a solid circular disk. Under these assumptions and under the further assumption of small linear perturbations about trim one obtains for zero advance ratio the following expressions for L and τ:

$$L = a\sigma/(2\gamma\,\bar{\nu}_o) \quad , \quad \tau = .113/\bar{\nu}_o \quad . \tag{2}$$

$a\sigma/2\gamma = .113$. Thus, according to the theory*

$$L = \tau = .113/\bar{\nu}_o \tag{3}$$

The average time mean induced flow was measured for 3 collective pitch angles in a plane .12R below the rotor, using hot wire anemometry. The results and the L and τ values from Eq. (3) are given in the following Table 3.

Table 3

θ_o°	$\bar{\nu}_o$	$\tau = L$
2	.016	7.0
5	.022	5.1
8	.033	3.4

*The relation between $\bar{\nu}_o$ and θ_o from the momentum theory is not satisfied and needs corrections from ground effects and from 3-dimensional flow effects (blade tip losses).

By comparing these values with those of Fig. 11 it is seen that for $\theta_o = 8°$ there is good agreement between the theoretical values of L and τ and those identified from transients. For $\theta_o = 2°$ and 5° the theoretical values for τ are too high. The equality of L and τ demanded by the theory also is not valid over the entire collective pitch angle range. Nevertheless, the simple theory can be used to establish approximate values for the rotor induced dynamic flow parameters. For example with $L = \tau = 4.5$ for $\theta_o = 5°$ one finds that the eigenvalue for the regressing flapping mode is changed by the dynamic inflow from $-.20 \pm 16j$ to $-.06 \pm .14j$, while the eigenvalue for the progressing flapping mode is hardly affected by the dynamic induced flow. Thus the damping of the regressing flapping mode is reduced by two thirds. Such changes are not limited to hingeless rotors with high P values and should have a noticeable effect on precision hovering. Reference 10 gives more data on eigenvalues.

Comparison with Frequency Response Tests

Extended frequency response tests with constant pitch stirring frequencies were conducted with the four-bladed rotor model, see reference 5. Figs. 12 a to c show for $\theta_o = 2°$, 5°, 8° respectively comparisons between analytical results based on the identified parameters and frequency response test results. The absolute values of the first harmonic Fourier coefficients for the induced flow (upper portion of Figs. 12 a, b, c) and for the flapping response (lower portion of Figs. 12 a, b, c) are plotted vs. the cyclic pitch stirring frequency. $+\omega$ values correspond to regressing, $-\omega$ to progressing cyclic pitch stirring.

An example of dynamic induced flow measurements made at 7 radial stations .12R below the rotor including the scatterbands ($\pm$ 1 standard deviation) is shown in Fig. 13. The assumption of a linear radial distribution is not well satisfied. The straight line distribution shown in Fig. 13 has the same moment about the rotor center as the measured distribution. Such straight lines were used to generate the data points (crosses) in the upper portions of Figs. 12 a, b, c. Though no flow measurements were used to establish the solid curves in Fig.s 12 a, b, c and though the presented flow data (crosses) are derived from inaccurate measurements, see Fig. 13, the agreement in the dynamic flow Fourier coefficients is reasonable. The experimental frequency flapping responses shown in the lower portions of Figs. 12 a, b, c agree even better with the analytical results.

Future Work

Research Contract NAS2-7613 has been extended through FY 1977. The following items, falling under either Research Goal (b) or Research Goal (c) listed in the Preface, are planned to be studied.

1. Cyclic Pitch Stirring Ramp Inputs. A mechanism has been built to impose cyclic pitch stirring ramp inputs. After the release of a spring the cyclic pitch stirring shaft is turned by an angle of 90 to 330 degrees. An energy absorber prevents the rebound of the shaft after impact on a stop. It is intended to compare the measured blade flapping response for this ramp input with the response computed with the identified perturbation model. Several hovering trim conditions and possibly forward flight trim conditions will be used.

2. State and Parameter Identifications from Forward Flight Trim Conditions.
   Contrary to hovering conditions, cyclic and collective flapping are coupled in forward flight. The question is whether the coupling is strong enough at low rotor advance ratio to identify states and parameters in the collective flapping perturbation equation from cyclic pitch stirring transients. Collective pitch transients may be needed, which are not feasible with the present wind tunnel rotor model. At higher advance ratio the simulations have shown that adequate collective - cyclic flapping coupling is available to perform a complete parameter identification from cyclic pitch stirring transients.
3. Extend Transient Testing to Higher Advance Ratio.
   At and beyond an advance ratio of .7 the tip path plane was observed to show indications of an impending instability. A new excentric with .5° amplitude has been made that can be substituted for the present 1.5° amplitude excentric. It is planned to retest high advance ratio conditions with the smaller excentric.
4. Extend the Perturbation Model to High Advance Ratio.
   The present perturbation model to be used for the state and parameter identifications neglects effects of reversed flow and of blade stall. In the high advance ratio region at least reversed flow effects must be included. It is likely that at high advance ratio the time constants for dynamic inflow in pitch and in roll may be different. The identification algorithm will be extended to the case of two separate cyclic inflow time constants.

5. Complete Construction of Hub Stirring Model. The construction of a hub stirring model is almost completed. It needs to be checked out and calibrated.

6. Test Hub Stirring Model. The hub stirring model will produce different blade flapping transients with higher coupling between collective and cyclic flapping. It is planned to test the model both for hovering and for forward flight trim conditions.

7. Elastic Blade Perturbation Model. So far the blades in the perturbation model have been assumed to be rigid and flexibly hinged at the rotor center. The blade natural flapping frequency could be easily and accurately identified from transient tests. It is planned to study at least by simulations some means to extend the identification method to elastic blades.

8. Sinusoidal Wind Tunnel Flow. A wind tunnel test section has been built that allows to produce sinusoidal up-or-down flow by oscillating vanes. A preliminary flow survey has been performed. If time and remaining funds allow, this tunnel test section will be used to produce transient normal flow variations at the rotor model. These transients could be used to identify the parameters in the collective flapping equation that are difficult to obtain from cyclic stirring transients at low advance ratio.

Conclusions

1. The state and parameter identification method previously selected (maximum likelihood identification) on the basis of computer simulated measurements could be simplified by using perturbations from trim with zero initial conditions of the states. Previously the initial cyclic pitch had been considered a perturbation from trim, which required initial value identifications.
2. An analytical model with identified equivalent Lock number shows much better agreement of the transient responses with the actual responses than an analytical model omitting rotor dynamic inflow. However, considerable response errors remain.
3. Both the test equipment and the data processing routine needed improvements. Non-uniformities in precone and prelag between the blades had to be removed. The resolver waves had to be reshaped. The cyclic pitch stirring acceleration capability had to be increased. Data handling could be improved by basing the identification algorithm on multiblade data rather than on single blade data. Measurement bias for the multiblade variables was additionally identified. The entire data processing and identification program was reformulated for use on the PDP-8 and PDP-12 mini computer complex with increased core memory, so that manual card punching was eliminated.
4. Minimum data length for the transients was found to be a critical requirement not only for the computer simulated but also for the actual measurements.

5. After appropriately modifying the test equipment, the input, and the data handling programs, the state and parameter identifications from cyclic pitch stirring transients from hovering trim conditions were highly successful. Convergence was rapid, the agreement between predicted and actual response very good, except for cases where the transients included high frequencies which the simple analytical model that is based on quasi-steady aerodynamics cannot properly represent.
6. Comparisons of the identified analytical perturbation models from hovering trim conditions with a simple theory showed reasonable agreement.
7. Comparisons of the identified perturbation models with frequency response test results showed good agreement in the flapping responses and reasonable agreement even in the quantitative description of the dynamic rotor inflow characteristics.
8. Future work will be mainly directed toward forward flight transient cyclic pitch stirring tests, toward higher advance ratio conditions, toward hub stirring tests, toward the inclusion of blade elasticity, and possibly toward the testing of the rotor model in wind tunnel flow transients.

References

1. Hohenemser, K. H. and Yin, S. K., "Methods Studies Toward Simplified Rotor-Body Dynamics", Part I of First Yearly Report under Contract NAS2-7613, June 1974.

2. Hohenemser, K. H. and Yin, S. K., "Computer Experiments in Preparation of System Identification from Transient Rotor Model Tests", Part II of First Yearly Report under Contract NAS2-7613, June 1974.

3. Hohenemser, K. H. and Crews, S. T., "Experiments with a Four-Bladed Cyclic Pitch Stirring Model Rotor", Part III of First Yearly Report under Contract NAS2-7613, June 1974.

4. Hohenemser, K. H., Banerjee, D., and Yin, S. K., "Methods Studies on System Identification From Transient Rotor Tests", Part I of Second Yearly Report under Contract NAS2-7613, June 1975.

5. Hohenemser, K. H. and Crews, S. T., "Additional Experiments with a Four-Bladed Cyclic Pitch Stirring Model Rotor". Part II of Second Yearly Report under Contract NAS2-7613, June 1975.

6. Hohenemser, K. H., Banerjee, D., and Yin, S. K., "Rotor Dynamic State and Parameter Identification From Simulated Forward Flight Transients", Part I of Third Yearly Report under Contract NAS2-7613, June 1976.

7. Hohenemser, K. H. and Crews, S. T., "Rotor Dynamic State and Parameter Identification From Hovering Transients", Part II of Third Yearly Report under Contract NAS2-7613, June 1976.

8. Crews, S. T., Hohenemser, K. H., and Ormiston, R. A., "An Unsteady Wake Model for a Hingeless Rotor", Journal of Aircraft, Vol. 10, No. 12, Dec. 1973, pp. 758-760.

9. Peters, D. A., "Hingeless Rotor Frequency Response with Unsteady Inflow", Rotorcraft Dynamics, NASA SP-352, 1974.

10. Ormiston, R. A., "Application of Simplified Inflow Models to Rotorcraft Dynamic Analysis", J. American Helicopter Soc., Vol. 21, No. 2, July 1976.

Figure Captions

Fig. 1 Normalized Standard Deviations vs. Duration of Cyclic Pitch Stirring Transient, $\dot{\omega} = -.10/\pi$.
$\sigma_\beta = .05$, $A = .50$, $AL/\tau = .25$, $1/\tau = .125$

Fig. 2 Noise Polluted Simulated Cyclic Pitch Stirring Input with Angular Acceleration $\dot{\omega} = -.10/\pi$, $\sigma_\theta = .1$

Fig. 3 Noise Polluted Simulated Blade Flapping Measurements for $\dot{\omega} = -.10/\pi$, $\sigma_\beta = .05$

Fig. 4 Cyclic Flapping Responses to Inputs from Fig. 2

Fig. 5 Cyclic Inflow Responses to Inputs from Fig. 2

Fig. 6 Test Input θ_{II} for Two Cyclic Pitch Stirring Accelerations

Fig. 7 Response for Slow Cyclic Pitch Stirring Acceleration.
Solid Line: $A = .39$, $L = 4.4$, $\tau = 4.6$;
Dash-dot-line: $A = A^* = .19$, $L = \tau = 0$;
Dash line: $A = .39$, $L = \tau = 0$;
Crosses: test points

Fig. 8 Responses for Fast Cyclic Pitch Stirring Acceleration.
Line symbols same as in Fig. 7

Fig. 9 Responses for Slow Cyclic Pitch Stirring Acceleration Beyond $t = 23$. Line symbols same as in Fig. 7

Fig. 10 Induced Flow Variables from Identified Rotor Model with $A = .39$, $L = 4.4$, $\tau = 4.6$

Fig. 11 Identified Induced Flow Parameters vs. Collective Pitch Angle

Fig. 12 a to c
First Harmonic Fourier Coefficient Amplitudes for Induced Flow and for Flapping Responses, $\theta_o = 2^o$, 5^o, 8^o respectively, $P = 1.17$

Fig. 13 Radial Distribution of First Harmonic Induced Flor for $\omega = -.067$, $\theta_o = 5^o$ at .12R below Rotor Plane

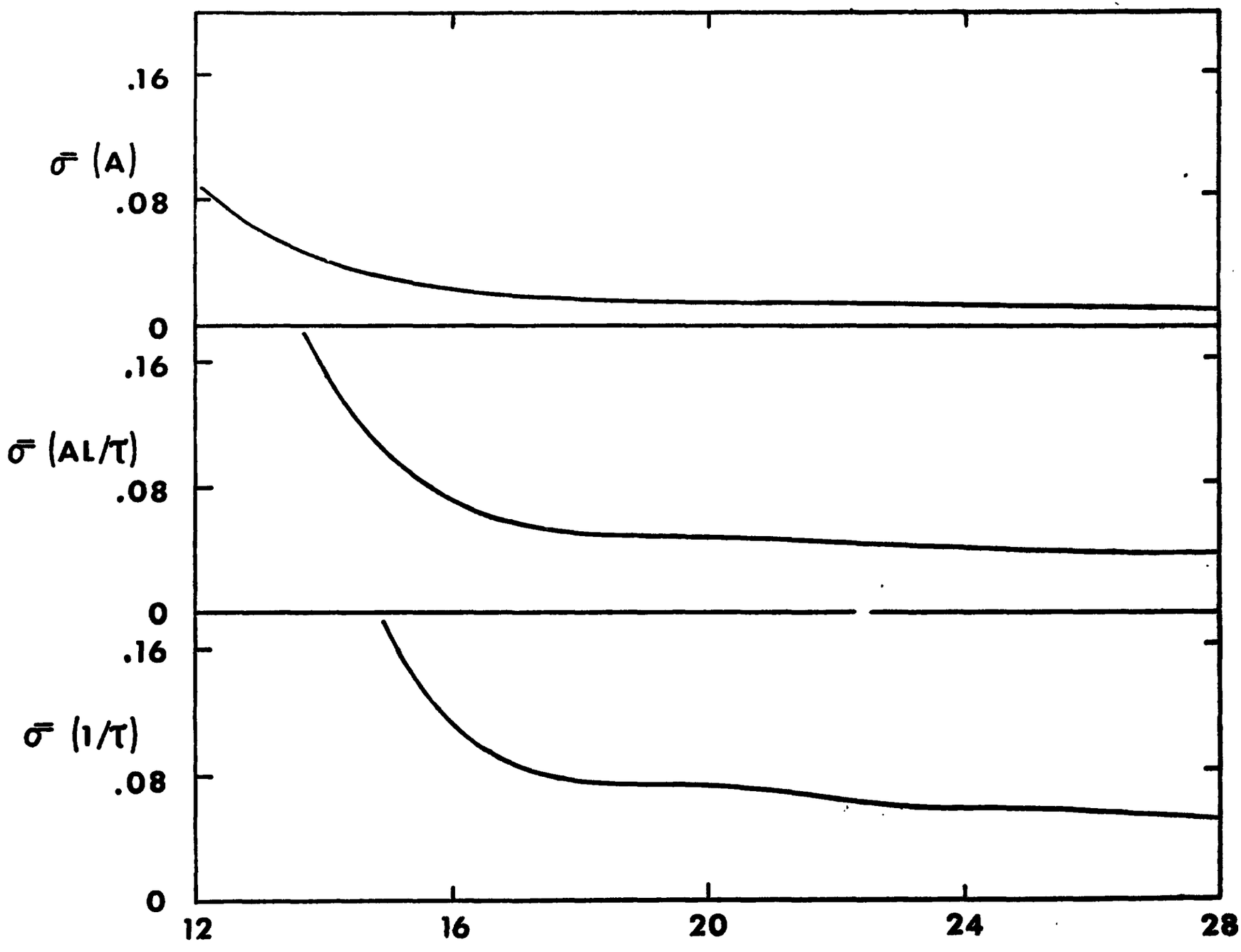

Fig.1

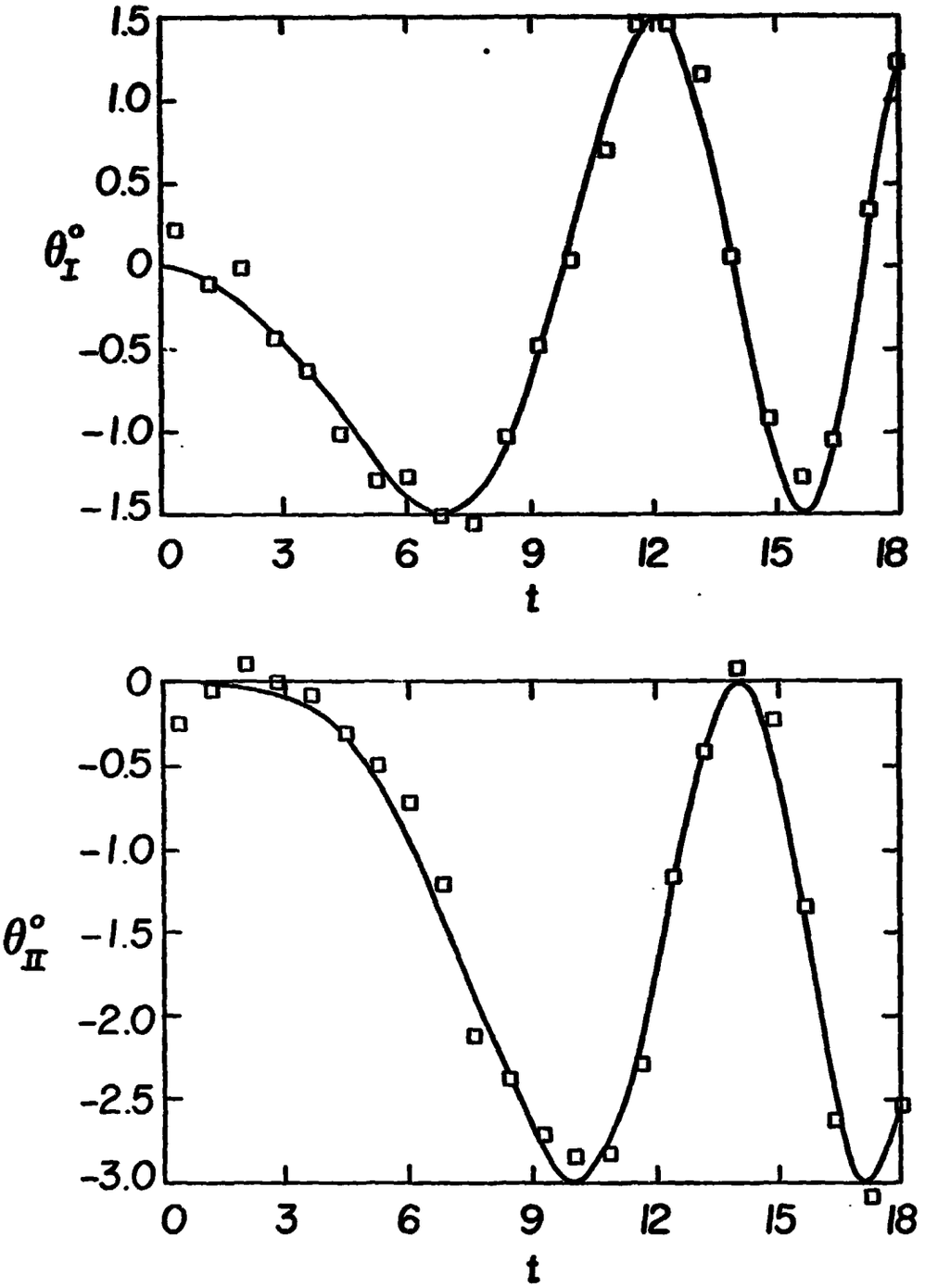
1.5
1.0
0.5
θ_I° 0
-0.5
-1.0
-1.5
0 3 6 9 12 15 18
t
0
-0.5
-1.0
θ_{II}° -1.5
-2.0
-2.5
-3.0
0 3 6 9 12 15 18
t

Fig. 2

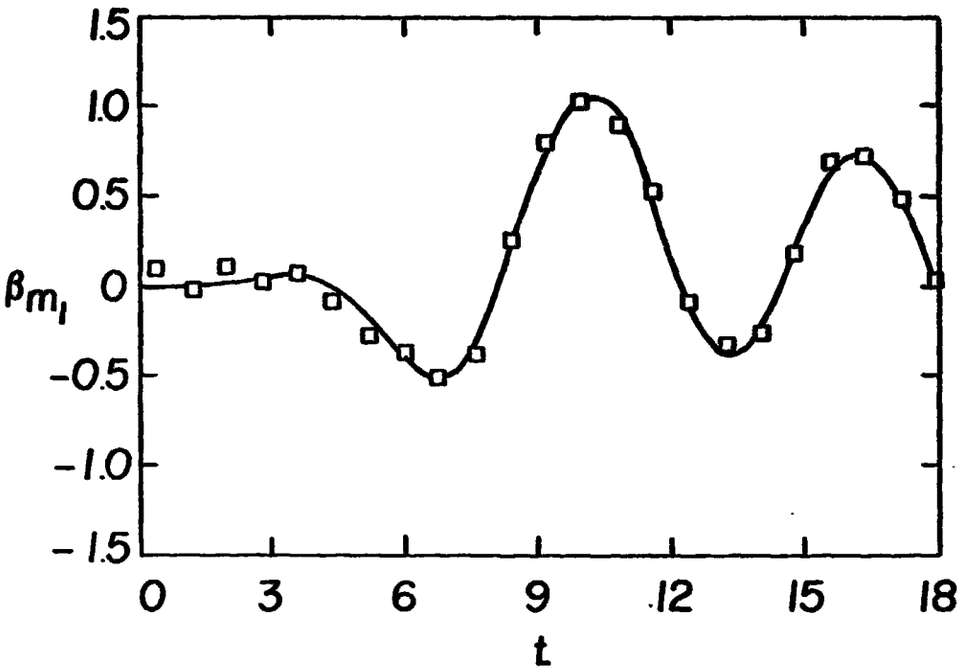
1.5
1.0
0.5
β_{m_1} 0
-0.5
-1.0
-1.5
0
3
6
9
12
15
18
t

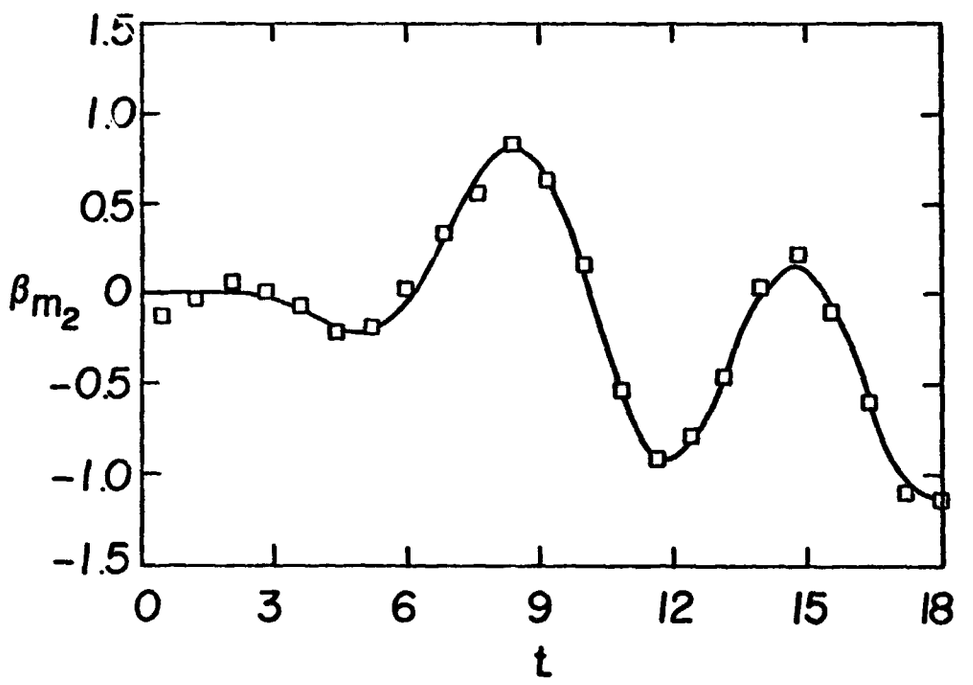
1.5
1.0
0.5
β_{m_2} 0
-0.5
-1.0
-1.5
0
3
6
9
12
15
18
t

Fig. 3

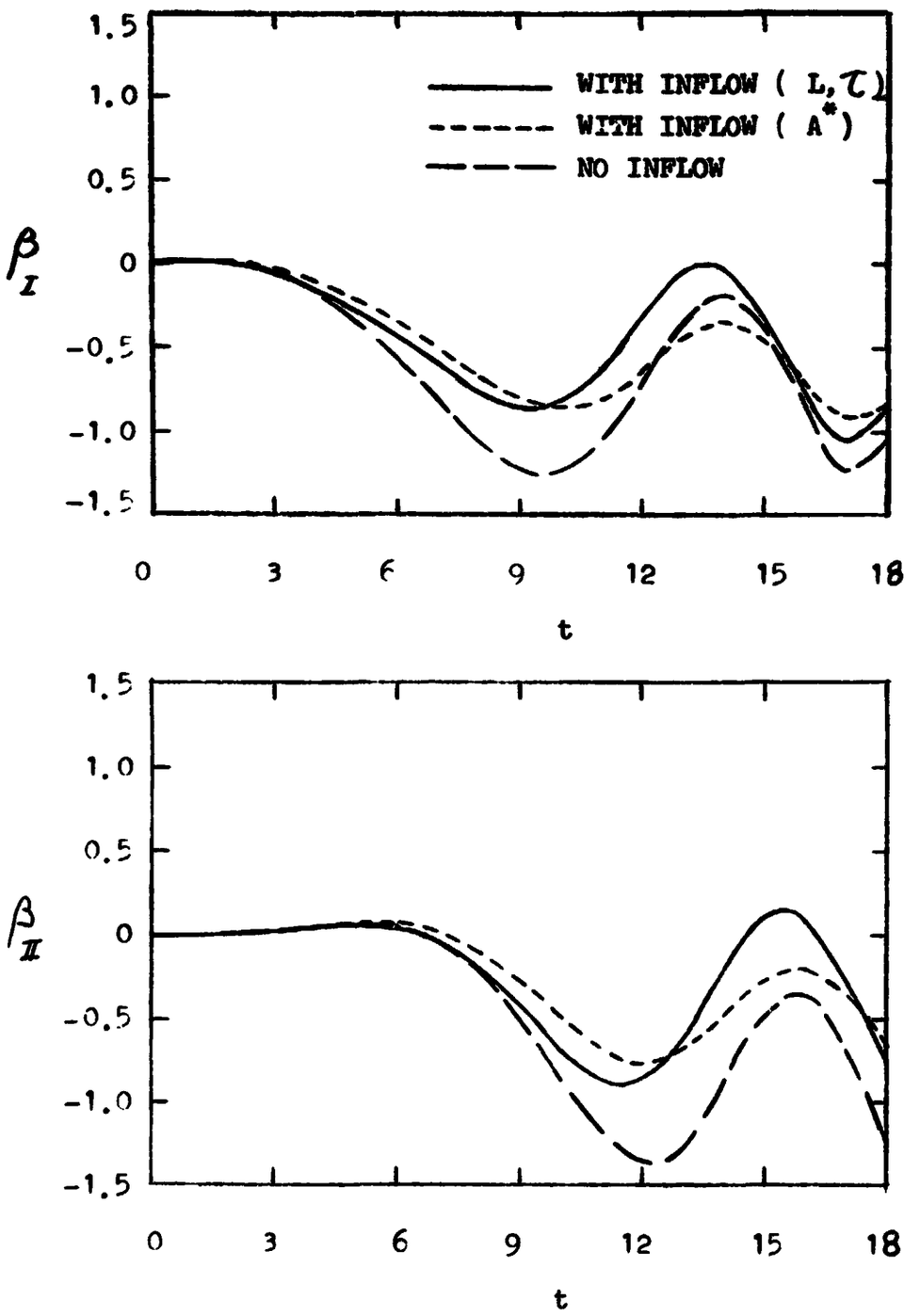
1.5
1.0
0.5
0
-0.5
-1.0
-1.5
β_I
WITH INFLOW (L, τ)
WITH INFLOW (A*)
NO INFLOW
0
3
6
9
12
15
18
t
1.5
1.0
0.5
0
-0.5
-1.0
-1.5
β_{II}
0
3
6
9
12
15
18
t

Fig. 4

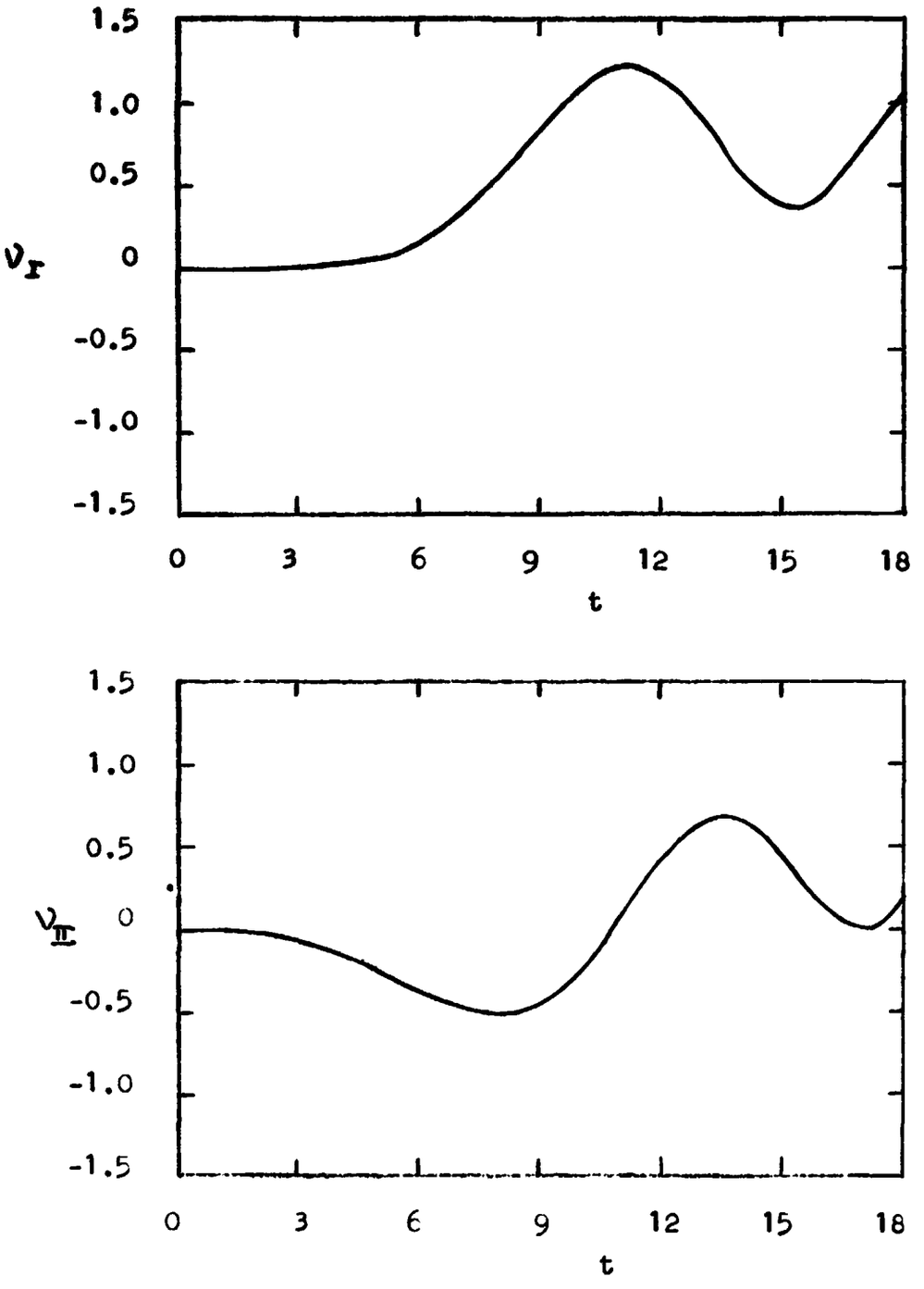

Fig. 5

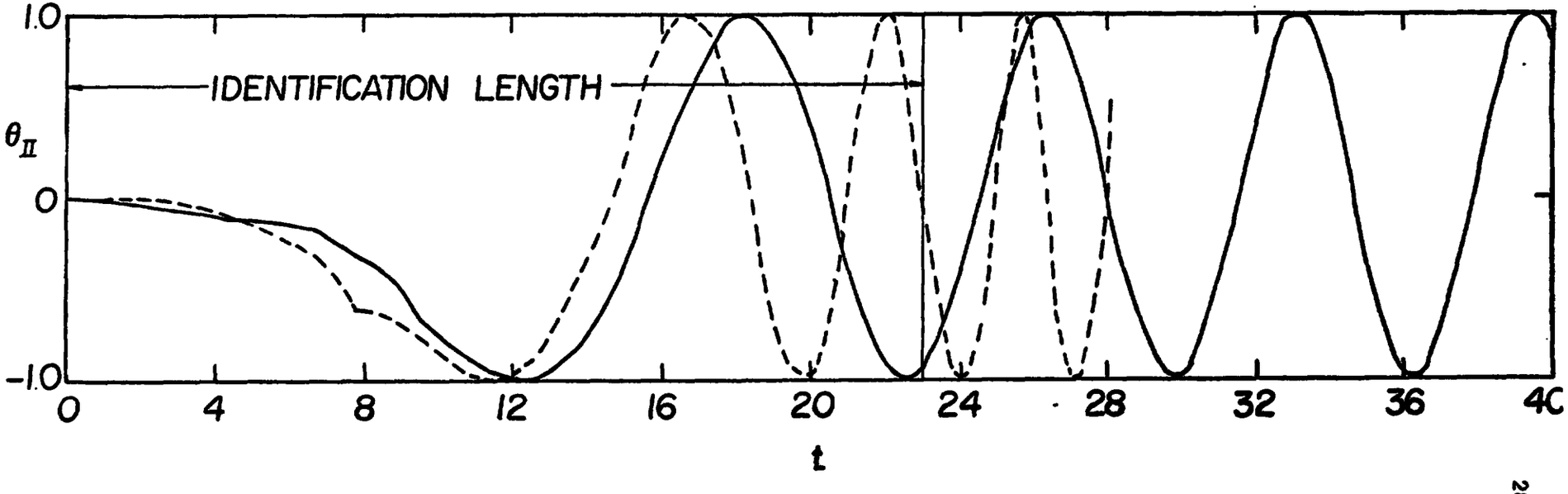
1.0
IDENTIFICATION LENGTH
θ_{II}
0
-1.0
0
4
8
12
16
20
24
28
32
36
40
t

Fig. 6

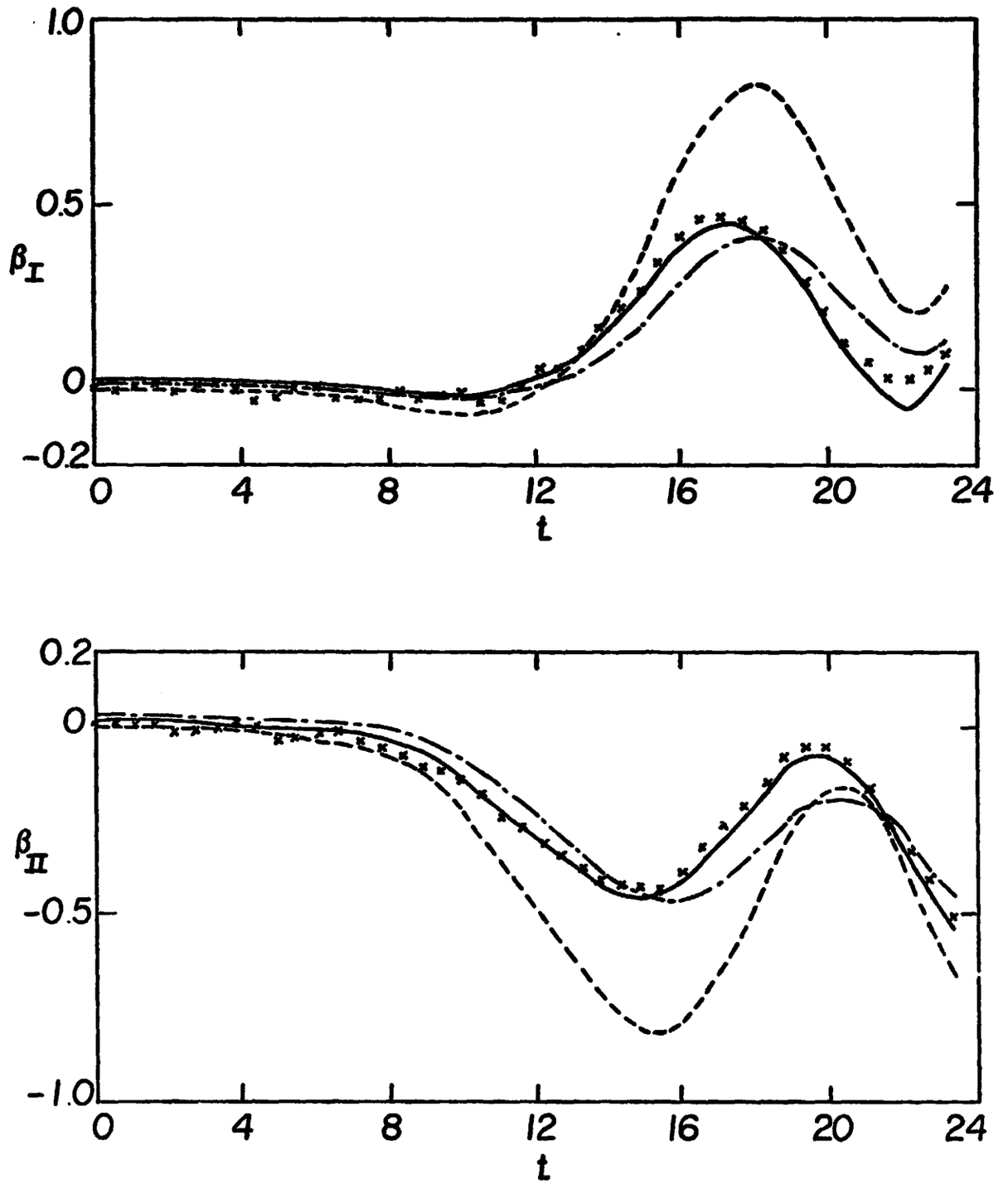

Fig. 7

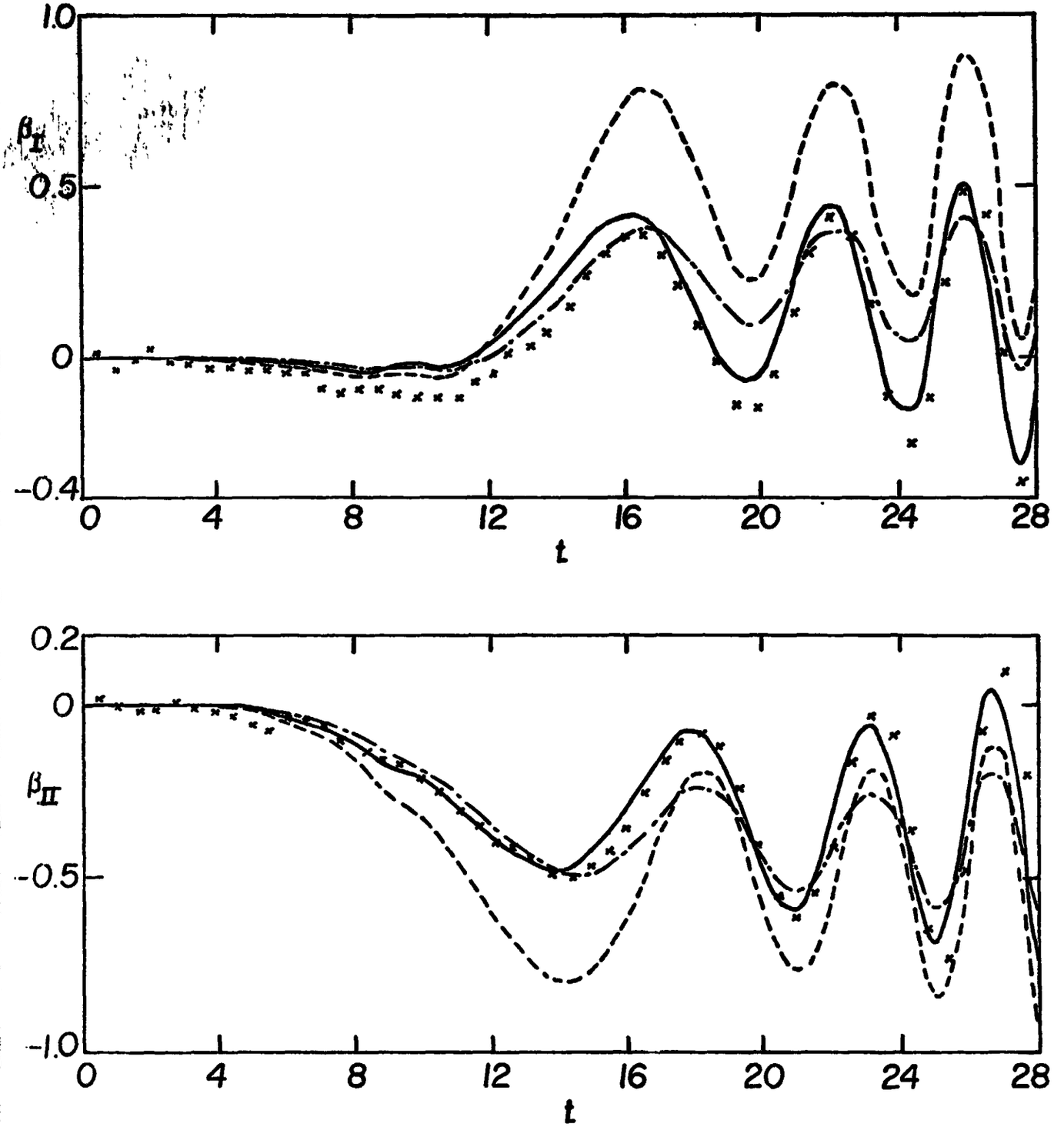
1.0
β_I
0.5
0
-0.4
0
4
8
12
16
20
24
28
t
0.2
0
β_{II}
-0.5
-1.0
0
4
8
12
16
20
24
28
t

Fig. 8

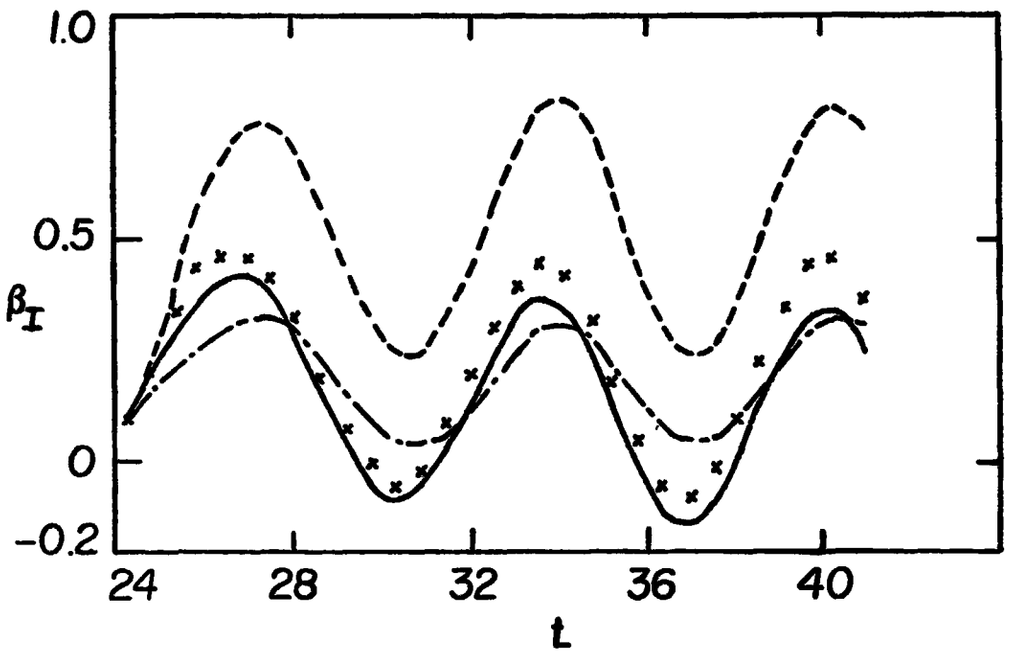

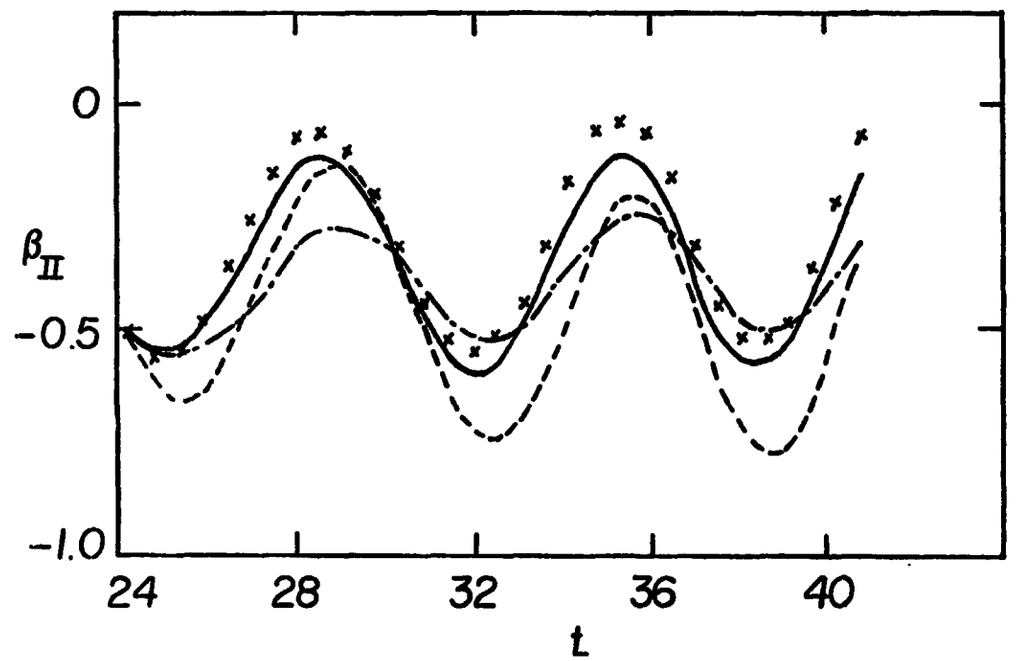

Fig. 9

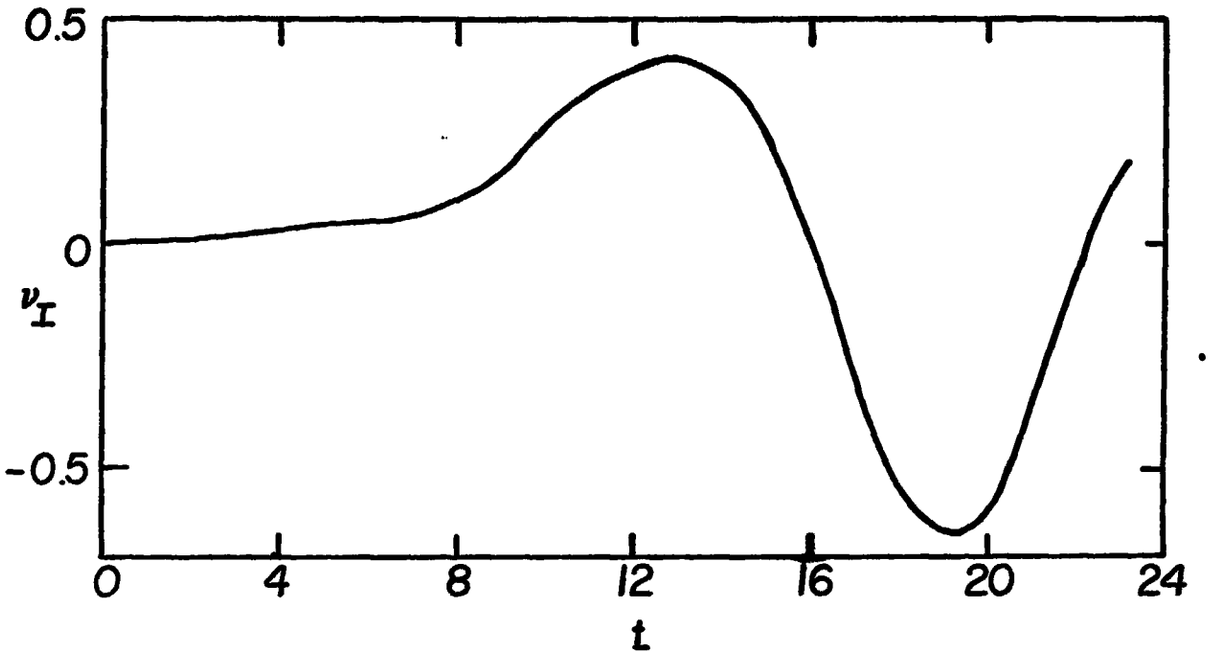

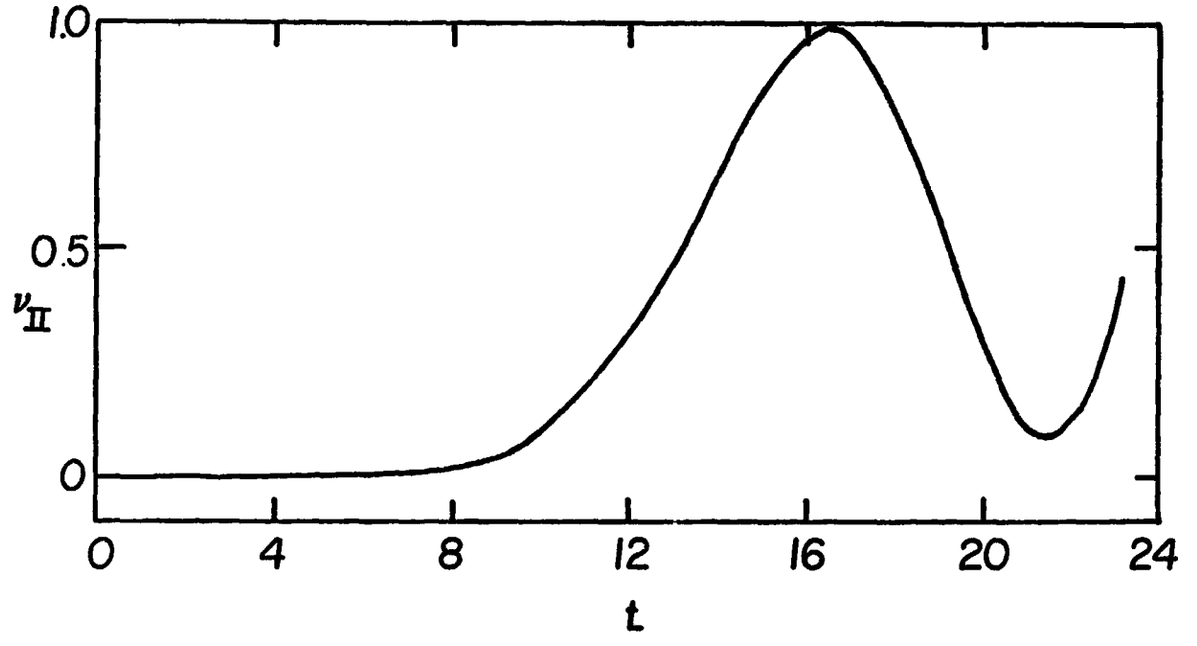

Fig. 10

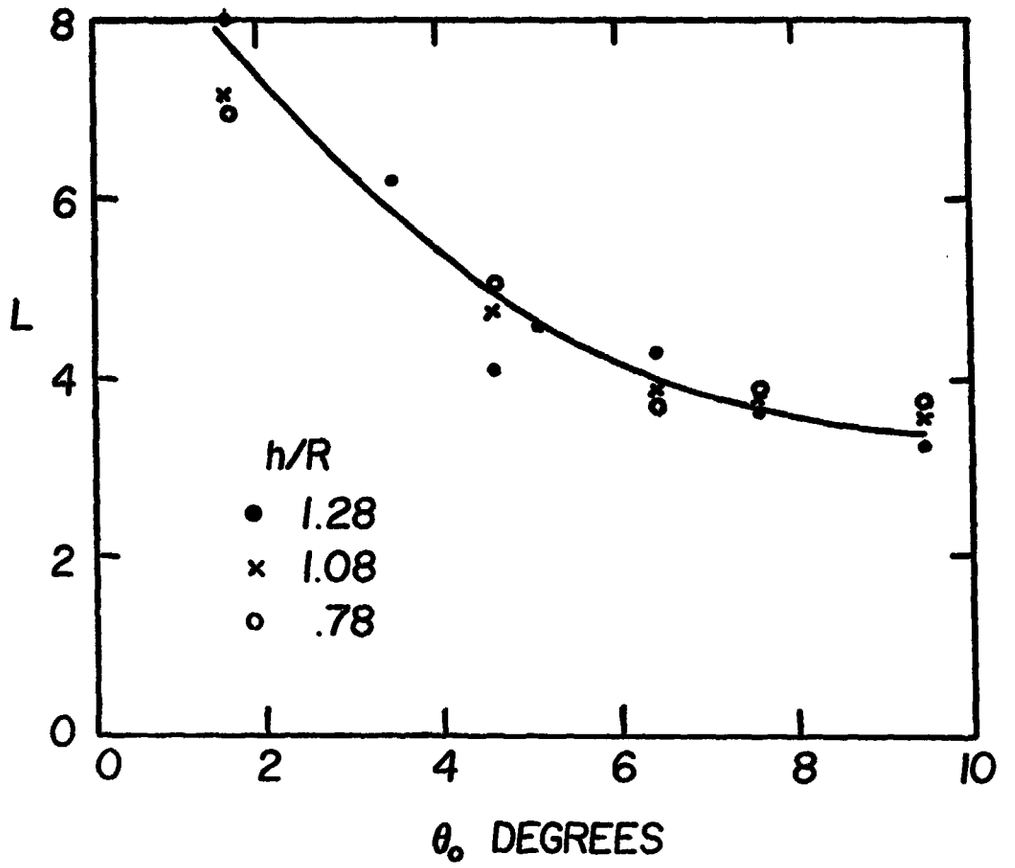
8
6
4
2
0
L
h/R
1.28
1.08
.78
0
2
4
6
8
10
θ₀ DEGREES

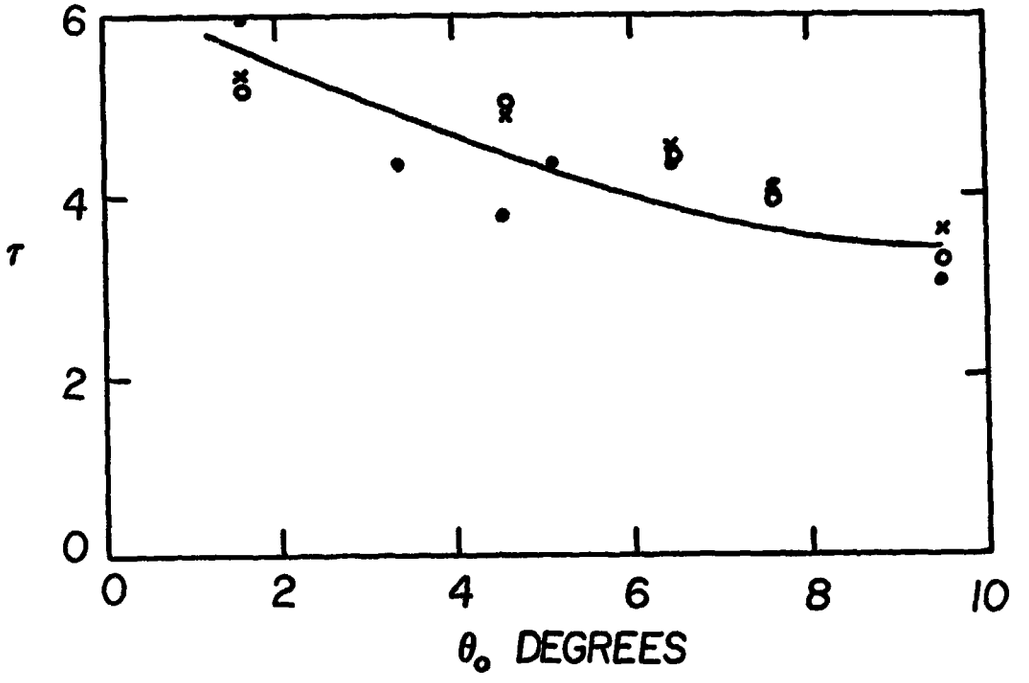
6
4
2
0
τ
0
2
4
6
8
10
θ₀ DEGREES

Fig. 11

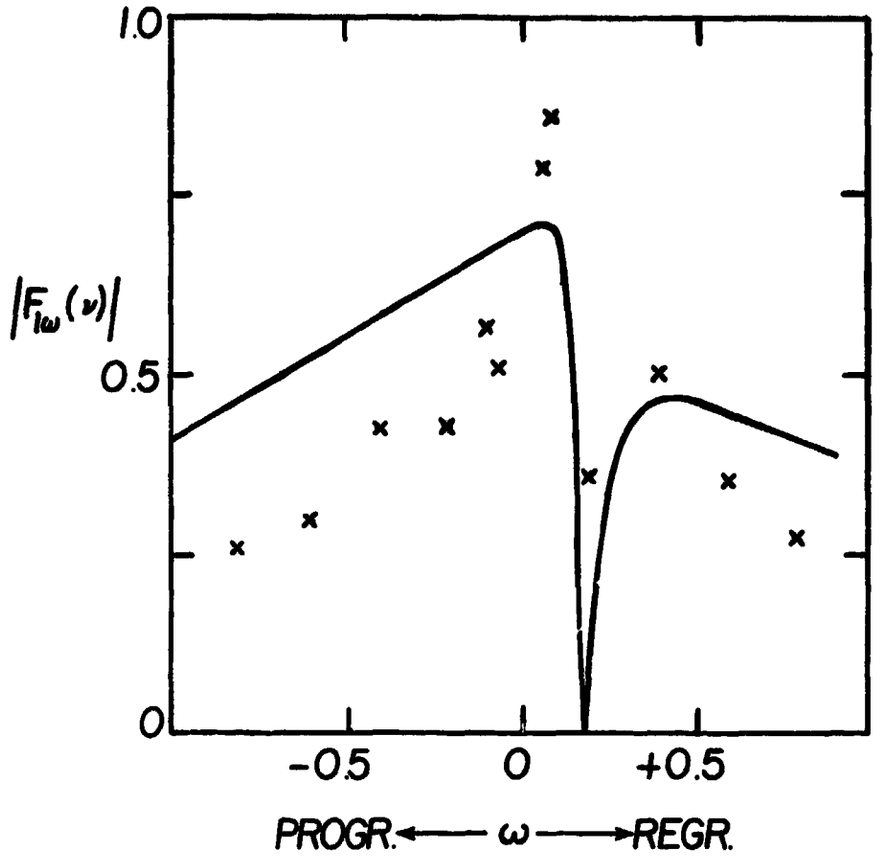
1.0
0.5
0
$|F_{1\omega}(\nu)|$
-0.5
0
+0.5
PROGR. ← ω → REGR.

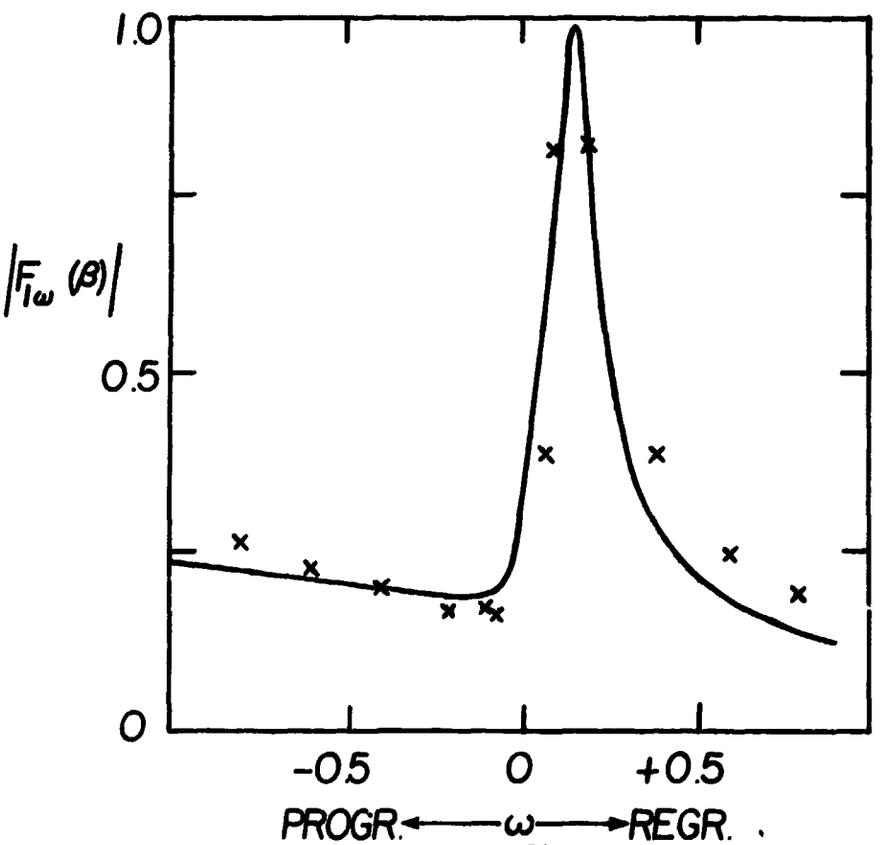
1.0
0.5
0
$|F_{1\omega}(\beta)|$
-0.5
0
+0.5
PROGR. ← ω → REGR.

Fig. 12a

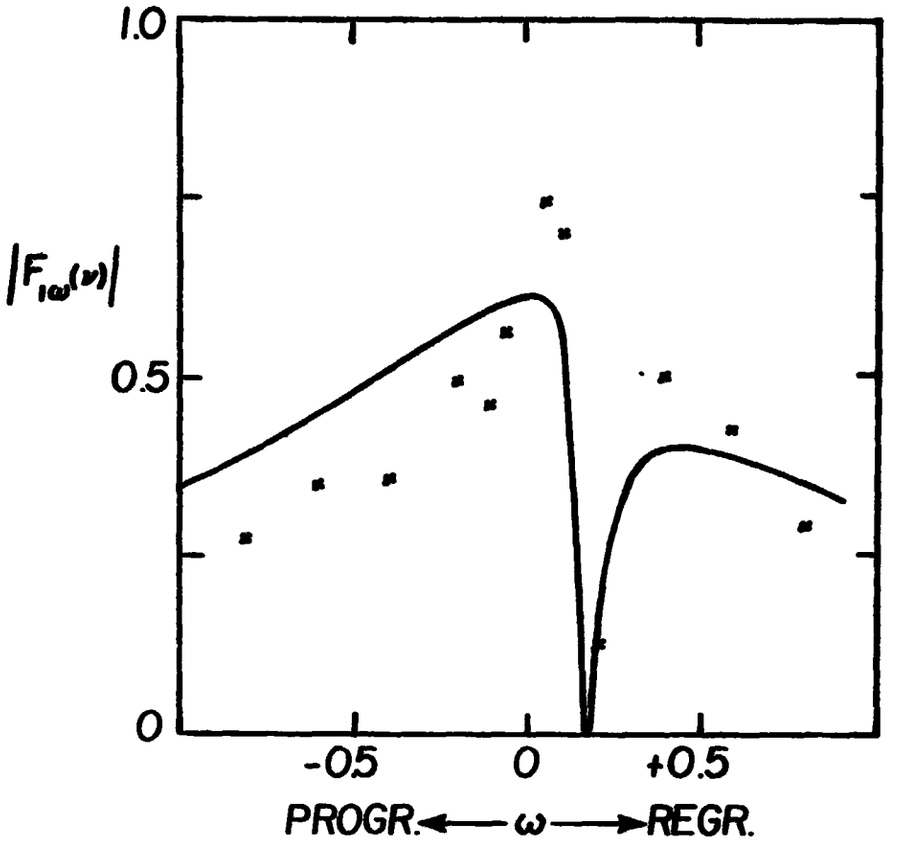

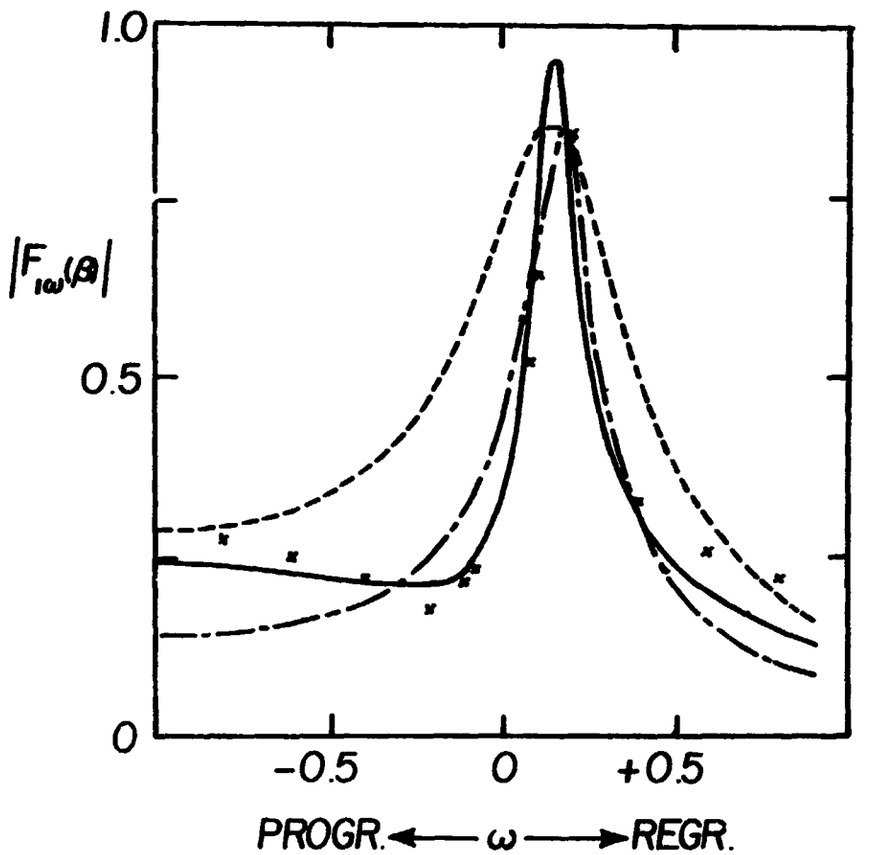

Fig. 12b

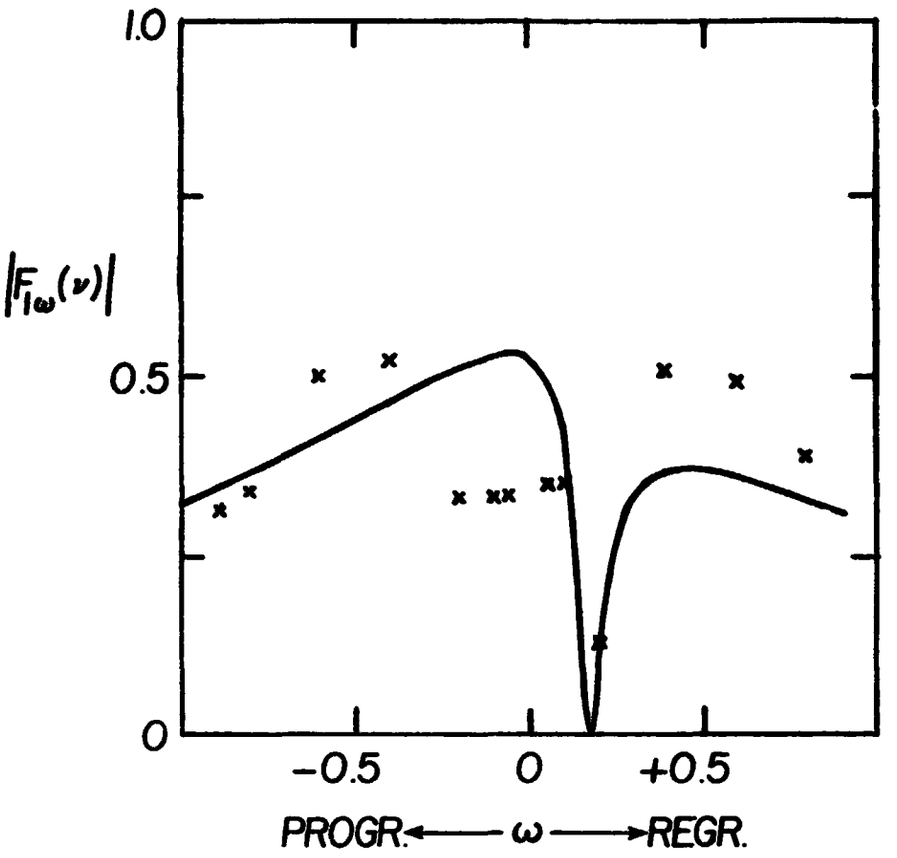
1.0
0.5
0
$|F_{1\omega}(\nu)|$
-0.5
0
+0.5
PROGR. ← ω → REGR.

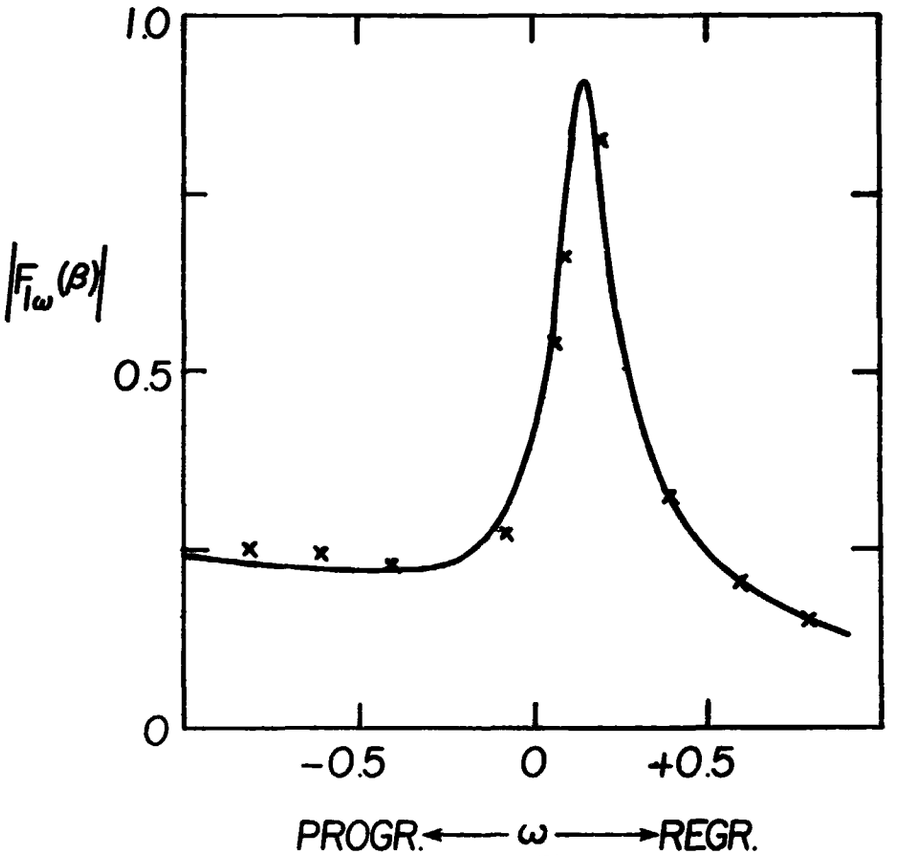
1.0
0.5
0
$|F_{1\omega}(\beta)|$
-0.5
0
+0.5
PROGR. ← ω → REGR.

Fig. 12c

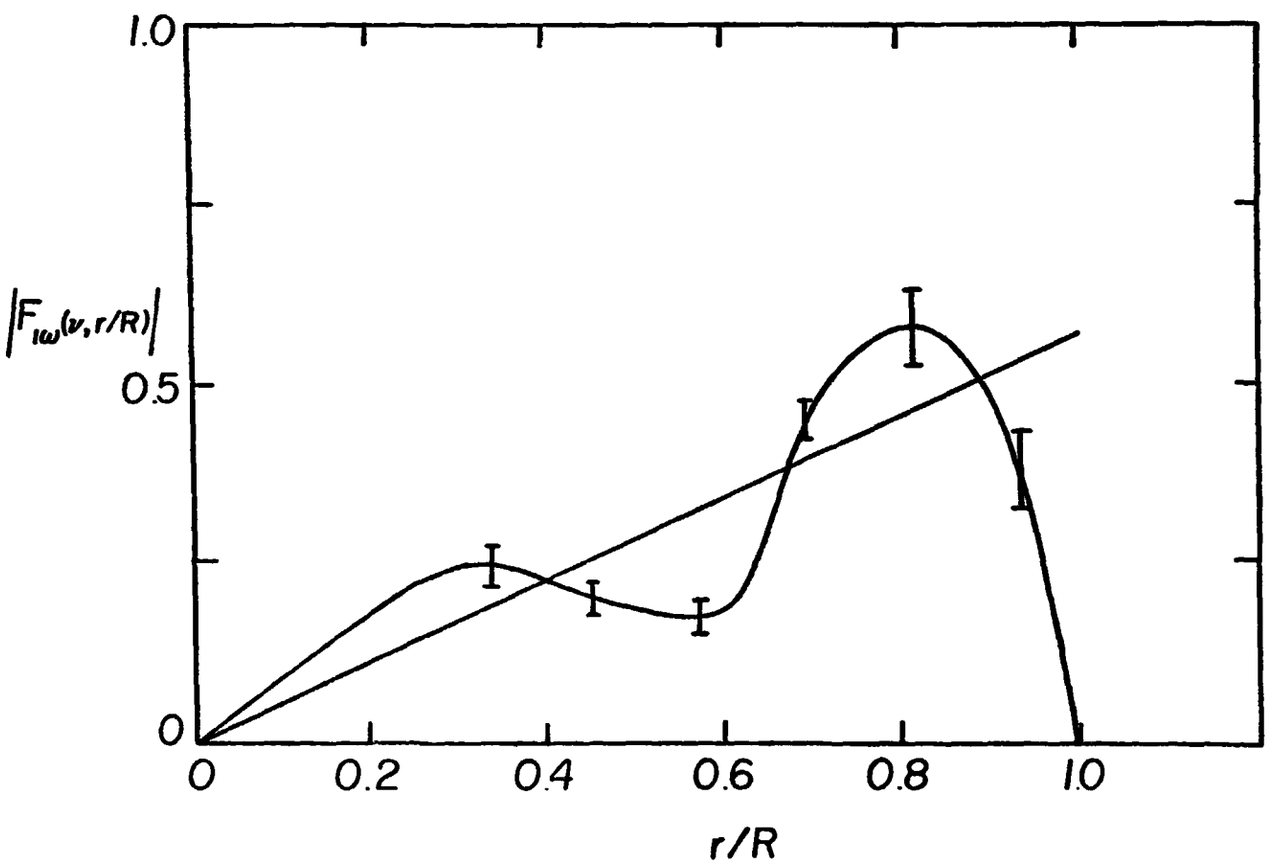

Fig. 13

Appendix A

List of Purchased and Borrowed Equipment

I Equipment purchased under Contract NAS2-4151 and carried over to Contract NAS2-7613

1. Items costing $500. to $1000.-

1 TSI Model 1057 Signal Conditioner	$ 645.-
1 TSI Model 1125 Calibrator	575.-

2. Items costing $1000.- and over

1 TSI Thermo Systems Inc. Model 1050 Research Anemometer	1,285.-
2 TSI Model 1052 Polynomial Linearizer at $1,150.- - each	2,300.-
1 TSI Model 1015C Correlator	1,075.-
	$5,880.

II Equipment purchased under Contract NAS2-7613

1. Items costing $500.- to $1000.-

1 EMI Laboratories 1540-9600 (Part of Stroboscope)	565.-

2. Items costing $1000.- and over
None

III Borrowed equipment over $1000.- New Value

1 TSI Single Channel Hot Wire Anemometry System	3,600.-
2 Tectronix Type 502A Dual Beam Oscilloscopes	2,200.-
1 Ampex FR-1300 Recorder/Reproducer	7,500.-
1 Hewlett Packard Thermal Recording System	7,500.-
1 Consolidated Electrodynamics Corp. Type 5-124 Recording Oscillograph	3,000.-
1 2-Channel Adjustable High-Low Pass Filter	2,200.-
	$26,000.